

Chemical networks and photoluminescence properties of carbon nanoparticles derived via sol-gel method

Umesh Rizal¹, Bhabani S. Swain², Bibhu P. Swain^{1*}

¹Nano-Processing Laboratory, Centre for Material Science and Nanotechnology, Sikkim Manipal Institute of Technology, Majitar, Rangpo 737136, East Sikkim, India

²School of Advanced Material Engineering, Kookmin University, Jeongnung-dong, Sungbuk-gu, Seoul, Korea

*Corresponding author, E-mail: bibhuprasad.swain@gmail.com

Received: 12 January 2016, Revised: 30 June 2016 and Accepted: 13 October 2016

DOI: 10.5185/amlett.2017.6423

www.vbripress.com/aml

Abstract

We have synthesized carbon nanoparticles (CNPs) via the sol-gel method using dextrose as carbon source with different concentration of ethanol. The effects of ethanol concentration (0.2 to 2.0 M) on the chemical network, electrochemical and photoluminescence properties of CNPs were examined using Fourier transform infra-red (FTIR) spectroscopy, Raman spectroscopy, cyclic voltammetry and photoluminescence (PL) spectroscopy. Field emission scanning electron microscopy (FESEM) image of CNPs shows CNPs of 40-80 nm were synthesized by sol-gel method. Chemical network study reveals the presence of various bonds such as C-H, C-H₂, C-H₃ and aromatic carbon present on the surface of the CNPs. Raman spectra shows that increasing of ethanol concentration decreases the crystalline size of CNPs. Cyclic voltammetry analysis shows prominent oxidation peaks at 0.1-0.2 V whereas the reduction peak observed at 0.2 V. The observed room temperature PL peak at 2.9 eV confirms a blue emission from CNPs. Copyright © 2016 VBRI Press.

Keywords: Carbon nanoparticles, chemical networks, cyclic voltammetry, photoluminescence.

Introduction

Carbon nanoparticles (CNPs) have attracted considerable research interest due to their application in adsorbents [2], composites [3], drug delivery [4], and medical imaging [5], energy storage application [6] and so on. Various techniques were employed for the synthesis of CNPs such as plasma assisted pulsed laser deposition method (PLD) [7], sol-gel method [8], acid treatment of castor oil seed [5], oxidation of candle soot [9], carbonization of carbohydrates [10], and electrochemical methods [11]. Shuskov et. al. reported spherical CNPs of diameter 80-100 nm grown via electric discharge of ethanol solution [12]. Gallego et. al. has synthesized nanostructured carbon by catalytic ethanol decomposition with the variation of ethanol/He flow rates from 10-50 ml/min [13]. Bhunia et al. have synthesized highly fluorescent CNPs with tunable visible emission from blue to red with variations of carbonization condition and processing temperature [10]. Porous CNPs with Micropores and Small Mesopores was synthesized carbonization of banana-peel followed by KOH activation [14]. Carbon nanoparticles synthesized by laser pyrolysis of hydrocarbons in a flow reactor have been investigated as a function of laser power [15]. Hollow fluorescent carbon nanoparticles with green emission were synthesized in single step process by simply mixing acetic acid, water,

and diphosphorus pentoxide [16]. Using H₂ and CH₄ in microwave plasma chemical vapor deposition, Yu *et al.* deposited CNPs which has comparable field emission properties as carbon nanotube [17]. Fluorescent carbon nanoparticles were synthesized by a facile, one-pot, low-temperature method with trypsin and dopamine as precursors [18]. Water-soluble carbon nanoparticles (CNPs) were fabricated by a facile, one step hydrothermal synthetic route using acid/alkali as additives [19]. Novel ultramicroporous carbon nanoparticles (UCNs) were synthesized by solvothermal polymerization of phloroglucinol and terephthaldehyde in dioxane at 220°C, followed by carbonization at 850°C [20]. Water-soluble fluorescent carbon nanoparticles were synthesized directly from active carbon by one step hydrogen peroxide-assisted ultrasonic treatment [21]. Carbon nanoparticles with a well-defined shape and a range of diameters between 50 nm and 300 nm have been synthesized from the pyrolysis of resorcinol formaldehyde copolymer [22]. Zhang et al reported high yields of hydrophilic carbon nanoparticles (CNPs) prepared by the controlled carbonization of sucrose [23]. In this article, we have synthesized CNPs from dextrose as carbon source in ethanol. We studied the structural, optical and electrochemical properties of CNPs by varying ethanol concentration. We correlate the structural properties by

ATR-FTIR and Raman spectroscopy to the optical properties of CNPs.

Experimental

Material

Dextrose, ethanol and sodium chloride (NaCl) were used as a precursor for the synthesis of carbon nanoparticles (CNPs). All the aqueous solutions were prepared using de-ionized (DI) water. The concentrations of ethanol solution were varied from 0.5 to 2.0M.

Methods

Dextrose was used as carbon source and alcohol/electrolyte as an additive. CNPs were synthesized directly from sol-gel method via a mixture of dextrose, ethanol and 0.5 M NaCl solution in DI water. In a typical procedure, 1 gm of dextrose was added into an ethanol solution of different concentration. Then the solution was stirred rigorously in a magnetic stirrer for 20 minutes. After that, the solution was transferred into beaker containing 50 mL of 0.5 M NaCl solution. The solution was then processed electrochemically in a three electrode system. The size and morphology of the CNPs samples were examined with field emission scanning electron microscopy (FESEM). Fourier transform infrared spectroscopy (FTIR-Perkin Elmer spectrometer) spectra were collected in transmission mode in the range 400-4000 cm^{-1} with a resolution of 1 cm^{-1} . The typical Raman spectrum of the CNPs was recorded by a Raman spectrometer (514.5 nm line of an Argon laser) at room temperature. Electrochemical measurements were performed with a CH instrument, potentiostat. The electrochemical cell was a standard three electrode cell operated at room temperature, featured an inlaid Pt disk as the working electrode, a platinum coil as the counter electrode, and a saturated calomel electrode as a reference electrode. Prior to each experiment, the working electrode was cleaned in 0.5 M H_2SO_4 solution, and then rinsed with de-ionized water to avoid error in analysis. The potential was applied between 0.5 V and + 0.5 V with a scan rate of 50 mV/s. Photoluminescence (PL) spectra were collected with a Perkin Elmer LS-45 fluorescence spectrometer with a Xe discharge lamp operating at room temperature. The excitation wavelength was varied from 300 to 360 nm.

Results and discussion

Morphology and microstructure

Fig. 1 shows the FESEM image of CNPs synthesized with 2 M ethanol. The spherical CNPs are distributed randomly and the diameter of CNPs varies from 40 nm to 80 nm. The CNPs remain in clusters; however, their surface is rough and porous. Ganeshwar et al. have observed spherical CNPs synthesized via sol-gel method using hydrochloric (HCl) acid as solvent [24]. They observed unusual non uniform structure of CNPs with different solvent medium [13]. Wang et al have observed monodispersed nanocubes and uniform nanospheres of CNPs [25].

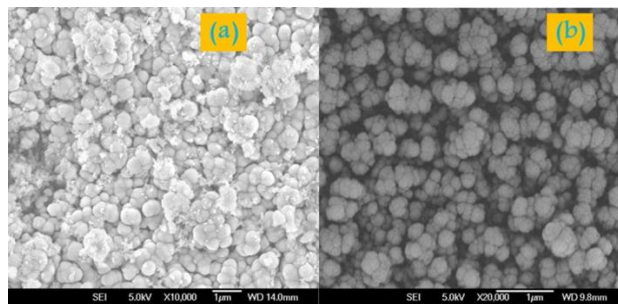


Fig. 1. FESEM of carbon nanoparticles at 2.0 M ethanol concentration.

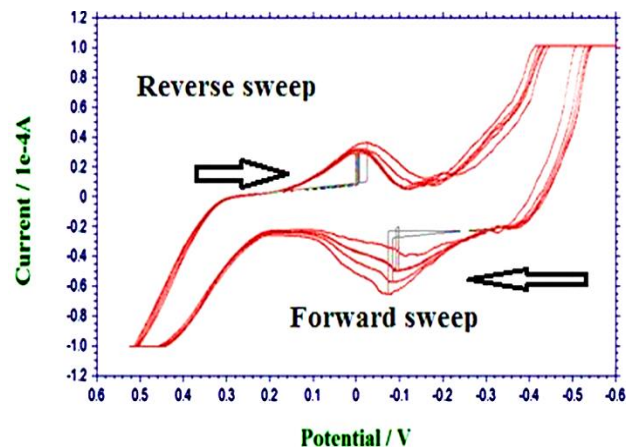


Fig. 2. Cyclic voltammogram of platinum electrode in 0.5 M NaCl solution 5 cycles.

Electrochemical characterization

Fig. 2 shows the cyclic voltammetry curves of platinum electrode in 0.5 M NaCl with a sweep rate of 50mV/s. We observe the typical oxidation peak at -0.074 V and the corresponding reduction peak at 0.001 V. In the region between the oxidation and reduction peak, the formation of double layer took place. However, a slight shift in oxidation and reduction peak was observed with increase in number of cycles. We have dissolved 1 gm of dextrose in different concentration of ethanol solution 0.5, 1.0, 1.5, 2.0 M respectively. After rigorous stirring, the ethanol dextrose solution was added into 0.5 M NaCl solution. Then, the solution was systematically connected with three electrode system. **Fig. 3 (a-d)** shows cyclic voltammetry curves of platinum electrode in different concentration of dextrose added in ethanol solution. The CV curves were with respect to saturated calomel electrode (SCE). From the figure, it can be seen that during forward sweep there are two oxidation peaks for platinum electrode at -0.25 V and $(0.1-0.2$ V) but there is one reduction peak for platinum electrode at 0.25 V during reverse sweep. As the number of cycle increases from 5 to 10, a gradual increase in cathodic and anodic current indicates progressive adsorption and desorption of reactive hydrocarbon monomers on the surface of CNPs. Shahrokhian et al. have studied the electrochemical behavior of Azathioprine at the CNP/N modified electrode surface. A sharp reduction peak was observed at -0.57 V indicates irreversible and adsorption like behavior of as synthesized CNP film [26]. Bok et al. revealed that an exponential increase of capacitance with decreasing

scan rates indicates the porous nature of CNPs [27]. Prasad et al. performed voltammetry studies of CNPs derived from castor soot. They observed that the working electrode in close association with CNPs exhibits increase in electrochemical activity towards various biological molecules as compared to unmodified electrodes [5].

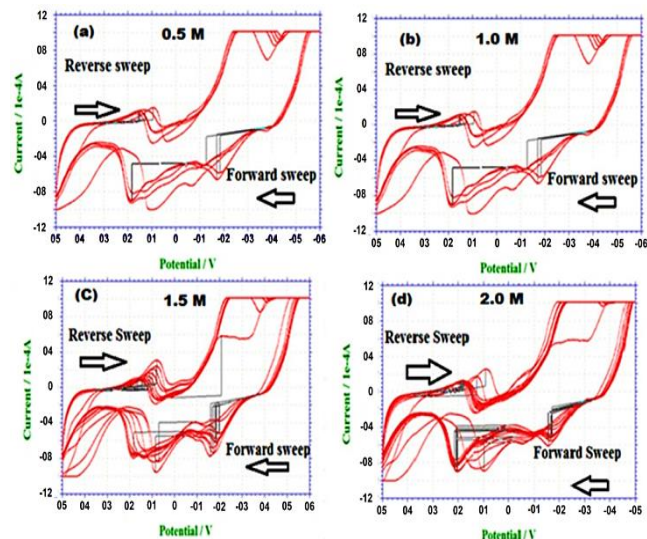


Fig. 3. Cyclic voltammogram of platinum electrode in different concentration of ethanol mixed with 1 gram dextrose in 0.5 M NaCl solution (a) 0.5 M ethanol (b) 1.0 M ethanol (c) 1.5 M ethanol (d) 2.0 M ethanol.

Bonding networks of CNPs

FTIR Spectroscopy

Fig. 4 shows the deconvolution of FTIR-ATR spectra of CNPs synthesized at different ethanol concentration. We observed various vibration peaks at 2669, 2792, 2859, 2935, 3080, 3204, 3275 and 3350 cm^{-1} correspond to the C-Cl, C-H, C-H₂, C-H₃, C-O, C-C-O, C=C-O and C=C=O stretching mode, respectively.

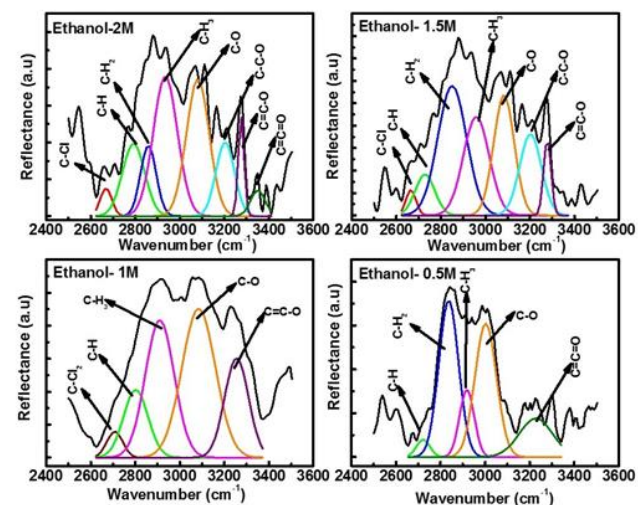


Fig. 4. Deconvolution of ATR spectra of CNPs synthesized with different ethanol concentration.

The vibration signature of different chemical constituents is identified based on their electronegativity

(C-Cl < C-H < C-H₂ < C-H₃ < C-O < C-C-O < C=C-O < C=C=O) and bond strengths. It can be clearly seen that the increase in the concentration of ethanol during the synthesis of CNPs results in increase in the bonding network of CNPs. Hossain et al. have observed peak at 2927 cm^{-1} for C-H stretch [28]. Hamaguchi *et al.* have observed three prominent vibrational signatures at 3410, 3027, 2927 cm^{-1} corresponds to the C-OH, CH (sp³), CH (sp²) respectively [29]. They also revealed that the presence or absence of a hydroxyl (-OH) group determines the hydrophilic or the hydrophobic character of the CNPs [28]. Li *et al.* have observed C-OH, C-H peaks at 3400, 300 cm^{-1} respectively. They revealed that the presence of O-rich hydrophilic groups on the surface of CNPs improves their luminescence properties [30]. Guo *et al.* have observed stretching vibration of hydroxyl groups spread over 3200-3600 cm^{-1} . On the basis of their FTIR spectra, they found that carboxylate and hydroxyl groups are present on the surface of CNPs [31]. Hu et al. have performed the IR characterization of their CNPs samples and found three prominent IR active signatures at 2960, 2876, 1380 cm^{-1} corresponds to CH₃ (assym), CH₃ (sym), δ (CH₃) respectively [32].

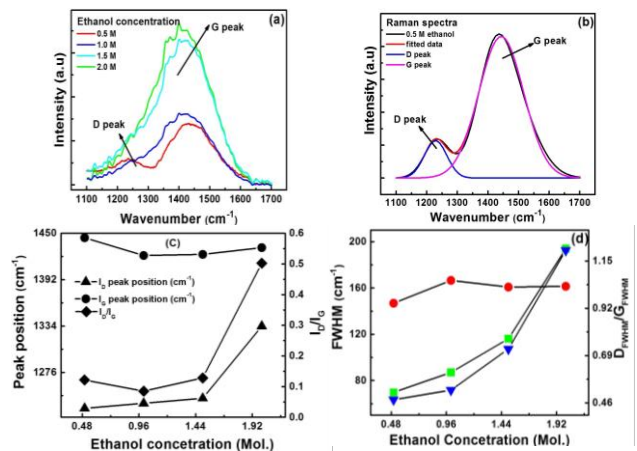


Fig. 5. (a). Raman spectrum of CNPs synthesized with different ethanol concentration, (b) deconvolution of Raman spectra of CNPs synthesized at 0.5 M ethanol concentration, (c) plot of peak position and I_D/I_G with different ethanol concentration, (d) plot of FWHM and D_{FWHM}/G_{FWHM} with different ethanol concentration.

Raman spectroscopy

Fig. 5(a) shows the Raman spectra of CNPs synthesized with different ethanol concentration. Various Raman signatures were appeared from 1100-1650 cm^{-1} . Two significant bands which peak were appeared at 1234.12 and 1416.73 cm^{-1} correspond to D band and G band respectively. The D peak arises due to the existence of sp³ coordination in the CNPs while G peak attributes to vibration mode involved with the in-plane bond-stretching motion of carbon bonds. It is evident from the figure that both peaks were appeared only for CNPs synthesized at 0.5 M ethanol concentration. However, at higher ethanol concentration, these peaks vanished and convoluted into one peak. Absence of doublet in the D and G peak is due to the formation of CNPs which resulted from overlapping of both bands in the Raman spectra. In order to distinguish the both band, the Raman spectra were

deconvoluted into two individual Gaussian peaks. **Fig. 5 (b)** shows the deconvolution of Raman spectra into two distinguished Gaussian peaks centred at 1229.2 and 1443.7 cm^{-1} corresponds to D peak and G peak for CNPs synthesized with different ethanol concentration. The diamond like carbon (DLC) peak is small with respect to graphitic carbon (GC) peak indicates more number of sp^3 carbon present in CNPs. The I_D / I_G ratio gives the idea about defect present in CNPs. **Fig. 5 (c)** shows the plot of the peak position and I_D / I_G with different ethanol concentration. The D peak and G peak shifted from 1231.2 to 1333.9 cm^{-1} and 1444.5 cm^{-1} to 1432.1 cm^{-1} with increasing of ethanol concentration from 0.5 to 2.0 M. The I_D / I_G varies from 0.121 to 0.502 indicates fewer defects present in the CNPs. As the I_D / I_G value is inversely with crystalline size of CNPs, therefore increasing of ethanol concentration decreases the crystalline size of CNPs. **Fig. 5 (d)** shows the plot of full width at half maximum (FWHM) and $D_{\text{FWHM}} / G_{\text{FWHM}}$ of CNPs synthesized with different ethanol concentration. The D_{FWHM} and G_{FWHM} increases from 69.81 to 194.03 cm^{-1} and 146.83 to 161.45 cm^{-1} , respectively, with increasing of ethanol concentration from 0.5 to 2.0 M. However, the ratio of $D_{\text{FWHM}} / G_{\text{FWHM}}$ is shifted from 0.475 to 1.2.

Optical Properties of CNPs

In order to study the optical properties of the CNPs, the room temperature photoluminescence (PL) spectra of the CNPs were recorded using a Xenon discharge lamp as an excitation source. **Fig. 6(a)** shows the PL spectra of CNPs synthesized with different ethanol concentration. The excitation energy was fixed at 330 nm (3.75 eV). The PL spectra of CNPs show a broad range of emission band between 2.5 to 3.2 eV with a main peak centred at 2.9 eV. We have also observed several peaks from 2.5 to 3.2 eV associated with different surface states. We identified five emission peak associated with different surface states centred at 2.67 eV (464 nm), 2.80 eV (442 nm), 2.84 eV (436 nm), 2.88 eV (430 nm) and 3.01 eV (411 nm). The origin of the luminescence is believed to be from the surface states related to the ligands on the surface of the CNPs [32].

This appearance of multiple bands could be due to the coordination of sp^3 carbon atoms with other elements, thus forming different carbon complex which were identified from the FTIR results. It is reasonable to assume that the solvent medium may introduce different defects centers on the surface of CNPs leading to various peaks. Tian *et al.* observed that the PL emission peaks becomes narrower after hydrothermal treatment which can efficiently passivate the defect centers from the surface of CNPs [33]. For more detail analysis, the PL spectra were recorded with varying excitation energy **Fig. 6 (b)** shows the PL spectra of CNPs with different excitation energy varies from 300 to 360 nm. The PL spectrum spreads over 2.0 to 3.5 eV with intense peak centred at 2.90 eV. The intense PL emission peak is observed when excited at 450 nm due to multi-photon active process and appearance of different PL intensity with different excitation wavelengths could be attributed

to different quantum yields. Li *et al.* have observed a strong PL emission peak of CNPs in visible region. They further observed the shift in PL peak towards longer wavelength region with increasing excitation wavelength [30].

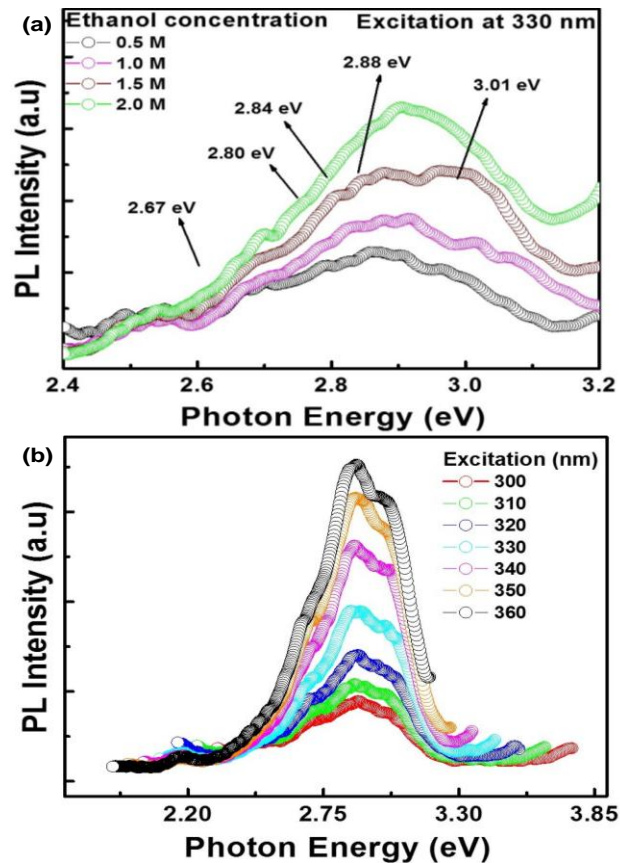


Fig. 6. (a) Room temperature PL spectra of CNPs with different ethanol concentration, (b) with different excitation wavelength.

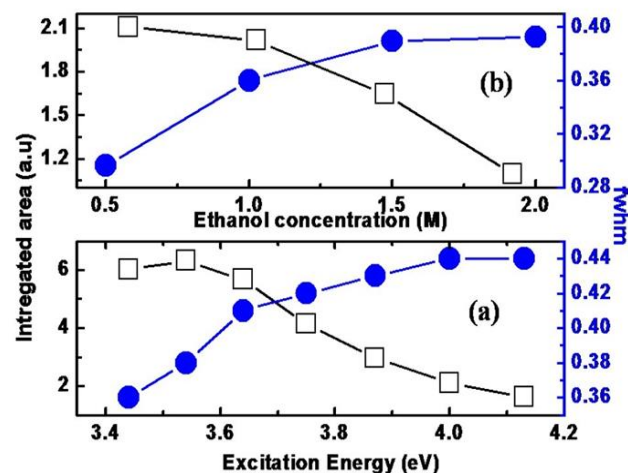


Fig. 7. Plot of integrated area and FWHM with (a) different excitation energy (b) different ethanol concentration.

Fig. 7(a-b) shows the plot of integrated peak intensity and their FWHM with different excitation energy and ethanol concentration. We observed that the integrated intensity decreases with increase in excitation energy and ethanol concentration while its FWHM increases from

0.36 to 0.44 and 0.29 to 0.40 eV. A decrease in the integrated PL signals implies non uniform distribution of defect states. A number of factors are associated with an increase or decrease of FWHM(a) size distribution of nanoparticles, (b) band filling effect of the localized states, (c) thermal broadening with increasing energy.

Conclusion

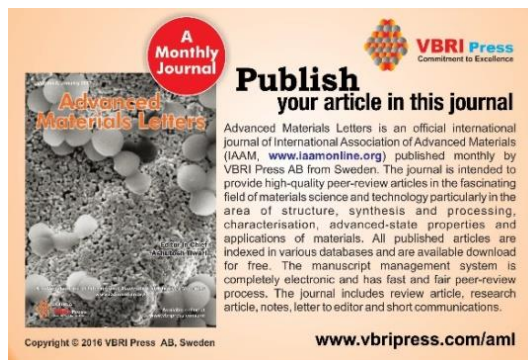
CNPs of diameter 40-80 nm were synthesized from dextrose source via sol-gel method. The chemical network modifications on the CNPs were tuned by the variation of ethanol concentration. I_D/I_G increases with increase in ethanol concentration confirmed decreases of crystalline size of CNPs with increasing ethanol concentration. Cyclic voltammogram of platinum electrodes showed prominent oxidation peaks at 0.1-0.2 V whereas reduction peak observed at 0.2 V respectively indicates adsorption of reactive methylene groups on the surface of CNPs. The presence of broad room temperature PL peak at 2.9 eV confirmed well defined blue emission from as synthesized CNPs.

Acknowledgements

The authors would like to thank AICTE (Project No: 20/AICTE/RIFD/RPS-POLICY-1), Government of India for providing financial support. Umesh Rizal thanks the Department of Biotechnology (DBT), India for providing fellowship.

References

- Schuster, J; He, G; Mandlmeier, B; Yim, T; Lee, K T; Bein, T; Nazar, L F; *Angew. Chem.*, **2012**, *51*, 3591.
DOI: [10.1002/anie.201107817](https://doi.org/10.1002/anie.201107817)
- Yue, Z R; Economy, J; J. Nanopart. Res., **2005**, *7*, 477.
DOI: [10.1007/s11051-005-4719-7](https://doi.org/10.1007/s11051-005-4719-7)
- Kato, M; Ishibashi M; *Journal of Physics: Conference series*, **2008**, *127*, 012003.
DOI: [10.1088/1742-6596/127/1/012003](https://doi.org/10.1088/1742-6596/127/1/012003)
- Kim, S; Shibata, E; Sergiienko, R; Nakamura, T; *Carbon*, **2008**, *46*, 1523.
DOI: [10.1016/j.carbon.2008.05.027](https://doi.org/10.1016/j.carbon.2008.05.027)
- Prasad, K S; Chuang, M C; Ho, J A; *Talanta*, **2012**, *88*, 445.
DOI: [10.1016/j.talanta.2011.10.056](https://doi.org/10.1016/j.talanta.2011.10.056)
- Chen T., Dai L. *Materials Today*, **2013**, *16*, 272.
DOI: [10.1016/j.mattod.2013.07.002](https://doi.org/10.1016/j.mattod.2013.07.002)
- Suda, Y; Ono, T; Akazawa, M; Sakai, Y; Tsujino, J; Homma, N; *Thin Solid Films*, **2002**, *415*, 15.
DOI: [10.1016/S0040-6090\(02\)00532-1](https://doi.org/10.1016/S0040-6090(02)00532-1)
- Zheng, G B; Sano, H; Uchiyama, Y; *Materials Science Forum*, **2013**, *750*, 188.
DOI: [10.4028/www.scientific.net/MSF.750.188](https://doi.org/10.4028/www.scientific.net/MSF.750.188)
- Ray, S C; Saha, A; Jana, N; R; Sarkar, R; *J. Phys. Chem. C.*, **2009**, *113*, 18546.
DOI: [10.1021/jp905912n](https://doi.org/10.1021/jp905912n)
- Bhunia, S K; Saha, A; Maity, A R; Ray, S C; *Sci. Rep.*, **2013**, *3*, 1473.
DOI: [10.1038/srep01473](https://doi.org/10.1038/srep01473)
- Zhang J., Shen W., Pan D., Zhang Z., Fang Y., Wu M., New J. *Chem.*, **2010**, *34*, 591.
DOI: [10.1039/b9nj00662a](https://doi.org/10.1039/b9nj00662a)
- Shuskov, S S; Genarova, T N; Leshchevich, V V; Penyazkov, O G; Gusakova, S V; Egorov, A S; Govorov, M I; Prismotrov, Y. A; *J. Engg. Phys and Thermophysics*, **2012**, *85*, 867.
DOI: [10.1007/s10891-012-0792-9](https://doi.org/10.1007/s10891-012-0792-9)
- Gallego, J; Gallego, G S; Daza, C; Molina, R; Barrault, J; Dupeyat, C. B; Mondragon, F; *Dyna*, **2013**, *80*, 78.
DOI: [dyna/v80n178/v80n178a10](https://doi.org/10.15446/dyna.v80n178/v80n178a10)
- Yang K., Gao Q., Tan Y., Tian W., Qian W., Zhu L., Yang C., *Chem. Eur. J.* **2016**, *22*, 3239.
DOI: [10.1002/chem.201504672](https://doi.org/10.1002/chem.201504672)
- Galvez A., Herlin-Boime N., Reynaud C., Clinarda C., Rouzaud J., *Carbon*, **2002**, *40*, 2775.
DOI: [10.1016/S0008-6223\(02\)00195-1](https://doi.org/10.1016/S0008-6223(02)00195-1)
- Fang Y., Guo S., Li D., Zhu C., Ren W., Dong S., Wang E., *ACS Nano*, **2012**, *6*, 400.
DOI: [10.1021/nn2046373](https://doi.org/10.1021/nn2046373)
- Yu J., Wang E. G., Bai X. D., *Appl. Phys. Lett.*, **2001**, *78*, 226.
DOI: [10.1063/1.1361286](https://doi.org/10.1063/1.1361286)
- Feng J., Chen Y., Han Y., Liu J., Ren C., Chen X., *Analytica Chimica Acta*, **2016**, *926*, 107.
DOI: [10.1016/j.aca.2016.04.039](https://doi.org/10.1016/j.aca.2016.04.039)
- He X., Li H., Liu Y., Huang H., Kang Z., Lee S-T., *Colloids and Surfaces B: Biointerfaces*, **2011**, *87*, 326.
DOI: [10.1016/j.colsurfb.2011.05.036](https://doi.org/10.1016/j.colsurfb.2011.05.036)
- Zhao Y., Liu M., Gan L., Ma X., Zhu D., Xu Z., Chen L., *Energy Fuels*, **2014**, *28*, 1561.
DOI: [10.1021/ef402070j](https://doi.org/10.1021/ef402070j)
- Li H., He X., Liu Y., Yu H., Kang Z., Lee S-T., *Mater. Res. Bull.*, **2011**, *46*, 147.
DOI: [10.1016/j.materresbull.2010.10.013](https://doi.org/10.1016/j.materresbull.2010.10.013)
- Vié R., Drahi E., Baudino O., Blayac S., Berthon-Fabry S., *Flex. Print. Electron*, **2016**, *1*, 015003,
DOI: [10.1088/2058-8585/1/1/015003](https://doi.org/10.1088/2058-8585/1/1/015003)
- Bao, L; Zhang, Z L; Tian, Z Q; Zhang, L; Liu, C; Lin, Y; Qi, B; Pang, D W; *Adv. Mater.*, **2011**, *23*, 5801.
DOI: [10.1002/adma.201102866](https://doi.org/10.1002/adma.201102866)
- Ganeshwar, P V; Sabarikirishwaran, P; *International Journal of Chem. Tech Research*, **2015**, *7*, 1465.
- Wang, Z; Li, F; Stein, A; *Nano. Lett.*, **2007**, *7*, 3223.
DOI: [10.1021/nl072068j](https://doi.org/10.1021/nl072068j)
- Shahrokhian, S; Ghalkhani, M; *Electrochem. Commun.*, **2009**, *11*, 1425.
DOI: [10.1016/j.elecom.2009.05.025](https://doi.org/10.1016/j.elecom.2009.05.025)
- Bok, S; Lubquban, A A; Gao, Y; Bhattacharya, S; Korampally, V; Hossain M; Gills, K D; Gangopadhyay, S; *J. Electrochem. Soc.*, **2008**, *155*, 91.
DOI: [10.1149/1.2868772](https://doi.org/10.1149/1.2868772)
- Hossain, M A; Islam, S; *Am. J. Nanoscience and Nanotech.*, **2013**, *1*, 52.
DOI: [10.11648/j.nano.20130102.12](https://doi.org/10.11648/j.nano.20130102.12)
- Hamaguchi, T; Okamoto, T; Mitamura, K; Matsukawa, K; Yatsuhashi, T; *Bull. Chem. Soc. Jpn.*, **2015**, *88*, 251.
DOI: [10.1246/bcsj.20140247](https://doi.org/10.1246/bcsj.20140247)
- Li, H; Ming, H; Liu Y; Yu, H; He, X; Huang, H; Pan, K; Kang, Z; Lee, S T; *New. J. Chem.*, **2011**, *35*, 2666.
DOI: [10.1039/c1nj20575g](https://doi.org/10.1039/c1nj20575g)
- Guo, Y; Wang, Z; Shao, H; Jiang, X; *Carbon*, **2013**, *52*, 583.
DOI: [10.1016/j.carbon.2012.10.028](https://doi.org/10.1016/j.carbon.2012.10.028)
- Hu, S L; Niu, K Y; Sun, J; Yang, J; Zhao, N Q; Du, X W; *J. Mater. Chem.*, **2009**, *19*, 484.
DOI: [10.1039/b812943f](https://doi.org/10.1039/b812943f)
- Tian, L; Song, Y; Chang, X; Chen, S; *Scripta materialia.*, **2010**, *6*, 883.
DOI: [10.1016/j.scriptamat.2010.02.035](https://doi.org/10.1016/j.scriptamat.2010.02.035)



Advanced Materials Letters
A Monthly Journal

Publish your article in this journal

Advanced Materials Letters is an official international journal of International Association of Advanced Materials (IAAM, www.iaamonline.org) published monthly by VBRI Press AB from Sweden. The journal is intended to provide high-quality peer-review articles in the fascinating field of materials science and technology particularly in the area of structure, synthesis and processing, characterisation, advanced-state properties and applications of materials. All published articles are indexed in various databases and are available download for free. The manuscript management system is completely electronic and has fast and fair peer-review process. The journal includes review article, research article, notes, letter to editor and short communications.

Copyright © 2016 VBRI Press AB, Sweden
www.vbripress.com/aml